40. Investigations on CRLH-TL based Multiband Conformal Antennas for Curved Surfaces

Mohammad Ameen, and Raghvendra Kumar Chaudhary

Department of Electronics Engineering, Indian Institute of Technology (Indian School of Mines), Dhanbad, India

mohammadmn61@gmail.com, and raghvendra.chaudhary@gmail.com

ABSTRACT

This paper discusses the design of a low profile and compact triple-band conformal antenna based on composite right/left-handed (CRLH) transmission line (TL). The intended antenna provides an electrically smaller size with ka = 0.84 due to its ZOR behaviour with complete electrical size of 0.17 λ0 × 0.20 λ0 × 0.004 λ0 at 2.27 GHz. The antenna provides a overall physical dimension of 23 × 27 × 0.6 mm3. The intended antenna provides three frequency bands ranging from (2.25–2.29 GHz), (3.39–3.95 GHz), and (4.80–6.12 GHz) with impedance bandwidths (IBWs) of 1.98%, 15.62%, and 24.95% for the three consecutive bands. The proposed CRLH-TL antenna exhibits a maximum gain of 0.76 dBi, 1.45 dBi, and 3.22 dBi for the three frequency bands respectively. The intended provides similar results for bending angle $\theta = 0^0$ to $\theta = 240^0$. Hence the intended conformal antenna is well suitable for working in various curved surfaces.

Index Terms— *composite right/left-handed, conformal antenna, triple band, low profile, transmission line.*

INTRODUCTION

Due to the emerging technologies and their corresponding applications, devices with lesser size and more number of functionalities are necessary for the upcoming and modern wireless application systems. Older antenna designs are based on microstrip planar structures, which faces the problem of smaller gain, higher cross-polar radiation, narrow impedance IBW, poor radiation efficiency with higher antenna dimensions. After the introduction of the metamaterials (MTMs), progressively technologies are showing drastic improvement in terms of antenna size and their performances. MTMs antennas are based on artificially engineered designs, which have both negative permeability ($\mu < 0$) and negative permittivity ($\varepsilon < 0$). These properties are shown by the LH structures with different features that are not achievable by existing RH structures [1]– [2].

MTMs can provide device miniaturization with good antenna performances, what the current technologies needed. MTM based antennas can be realized either by CTLH-TL based structures [1–10] or resonant approach [11–12] by the placement of split-ring resonator (SRR), complementary SRR, and so on. The inherent features of MTM are the generation of negative order mode, ZOR modes and first-order mode which are being exploited for device miniaturization with multiple numbers of operating frequency bands [1]. Different types of MTM based antenna configurations are highlighted with wideband and multiband performances are explained in [2–15], where it mainly uses CRLH-TL based wideband antenna by merging different modes [3–5], epsilon negative -TL based narrowband CP antenna [6], ENG-TL with square-shaped crossed slots [7], CRLH-TL based wideband antennas [8], loading of two simplified MTM transmission lines [9], loading of multiple CRLH-unit cells [10], complementary capacitive loops [11], MTM inspired antenna using SRR [12], patch loaded with electromagnetic bandgap conductor [13], and ENG-TL based MTM inspired antenna [14]. Besides the advantage of compactness and wider bandwidth, these antennas facing the problem of lesser gain [8], [10], [14]. and lower radiation efficiency [10] with a larger antenna profile [5], [14].

Recently, the use of conformal antennas are also getting more interest towards the antenna designers and researchers due to the reason of easily mountable to any curved surfaces and it provides design flexibility by changing the bending angle (θ). Various number of conformal antennas based on MTM [15], as well as microstrip technology [16–19] are explained in the literature. Antennas based on epsilon negative zero and munegative zero explained [15], conformal array [16], flexible antenna with reconfigurability [17], loading MTM structures [18] and multiple-input-multiple-output antenna based on conformality [19]. These antennas provide better results at

the expense of larger size and volume. Hence it is difficult to arrange properly on the newer application systems. Even though these antennas facilitate moderate IBW, but they do not provides compactness and required gain for the contemporary technology needs. The current antenna designs are targeted towards compactness and lesser space utilization. Hence it is necessary to design a flexible antenna with better performance that is useful for the modern wireless application systems.

In this work, a CRLH-TL based low-profile antenna is motivated from [2] is made into a conformal antenna for tripleband applications is investigated. The antenna compactness is achieved due to the CRLH-TL property. The newly designed MTM antenna can be used in various curved surfaces by changing the $\theta = 0^0$ to $\theta = 240^0$. The intended antenna without bending can covers almost similar response when compared with conformal for various bending angles.

ANTENNA GEOMETRY AND DESIGN

The simplified view of the designed triple band CRLH-TL loaded antenna with dimensions are marked as depicted in Fig. 40-1. The intended CRLH-TL antenna geometry is designed on the antenna fabrication is not complex. The intended CRLH-TL antenna mainly exists of an upturned 'L' shaped feed line of length (Lf1 + Lf2 + G2) and width (Wf). A trimmed step-shaped slot of width G2 is placed inside the main feed line, which gives the CRLH-TL series capacitance (CL) [1]. A chamfered meander line is added for achieving the shunt elements LL and CR. The edge chamfered meander line is connected with a corner blended triangular-shaped stub for providing the virtual ground to CRLH-TL. Fig. 40-2 demonstrates the 3D view of the actual antenna ($\theta = 2100$) designed for different faces of the front view. The final dimensions of the CRLH-TL antenna with $\theta = 00$ are 23 × 27 × 0.6 mm3 with electrical size of 0.17 λ0 × 0.20 λ0 × 0.004 λ0 at 2.27 GHz. The optimized dimensions at $\theta = 00$ are L = 23, L1 = 6, L2 = 0.35, LV = 6.92, Lf1 = 8.5, Lf2 = 18.20, Lg = 5, W = 27, W1 = 1.8, W2 = 9, Wg = 17.7, Wf = 5, G1 = G2 = 0.3, and G3 = 0.5 (All dimensions are in mm).

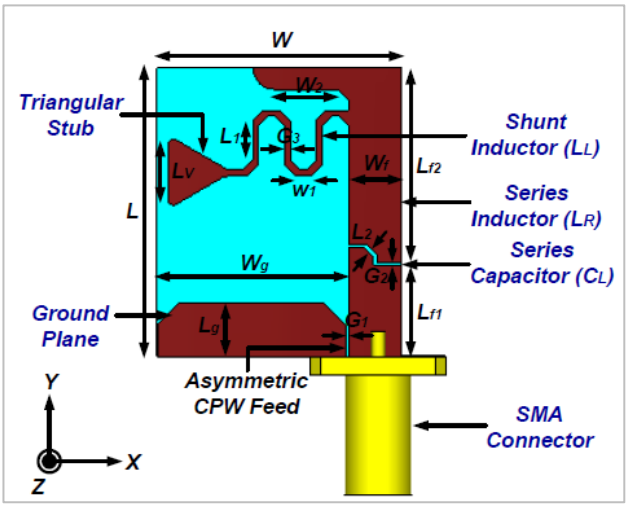

Figure 40-1 The schematic view of the proposed tri-band antenna modified from [2].

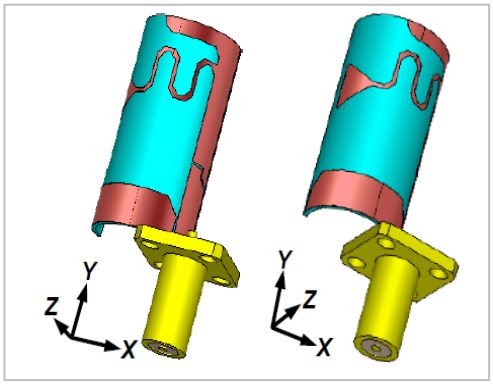

Figure 40-2 The 3D view of the conformal antenna for different angles of front view

A. DESIGN STAGES OF THE PROPOSED ANTENNA

Fig. 40-3 and 40-4 displays the design evolution stages of the intended CRLH-TL antenna and its input reflection coefficient responses (S_{11}). Firstly, a microstrip line and ground plane uses asymmetric CPW feeding which is represented as Antenna 1. The continuation of the microstrip feed line to an upturned '*L*' shape feed denoted as Antenna 2 in Fig. 40-3(b). The addition of step-type capacitor, meander lines, and triangular strip results in the generation of CRLH-TL antenna-3 in Fig. 40-3(c). In the next stage, modifying the trimmed shape meander lines

and step-type capacitor results in antenna-4 is plotted in Fig. 40-3(d). In the last stage, changing the bending angle $\theta = 0^0$ to $\theta = 210^0$ results in Antenna-5 depicted in Fig. 40-3(e).

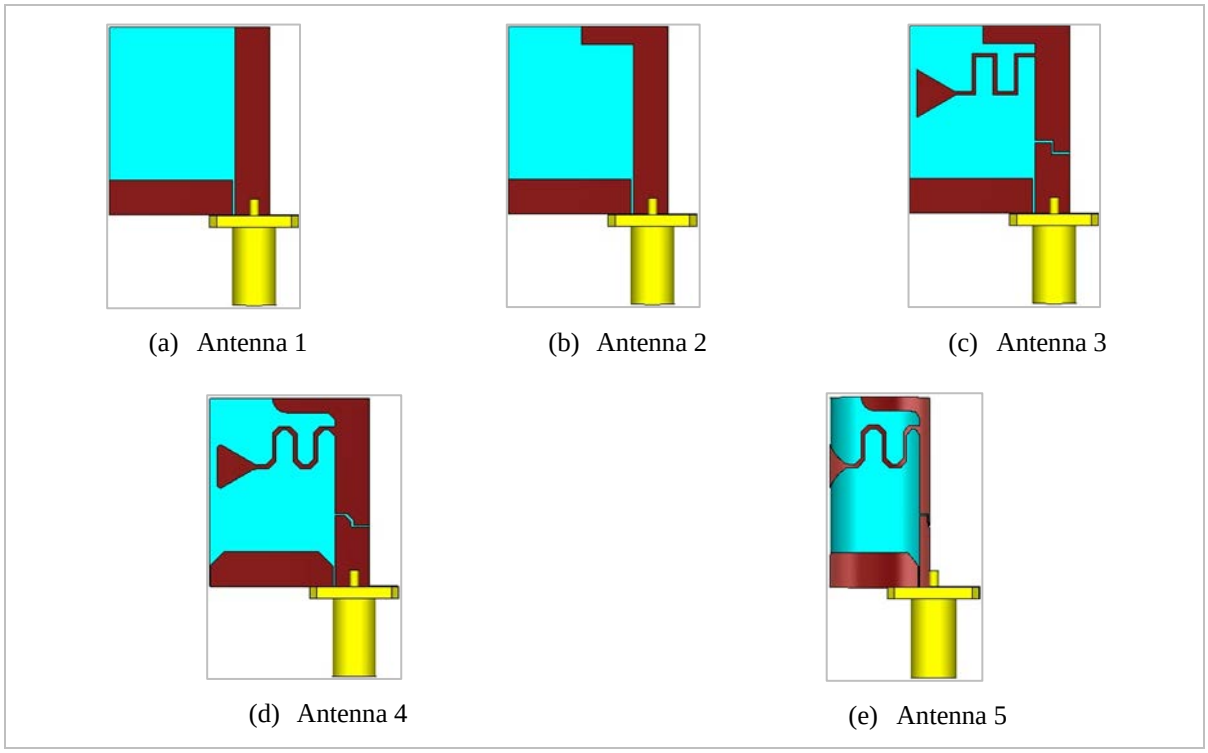

Figure 40-3 The conformal antenna design evolution from Antenna-1 to Antenna-5.

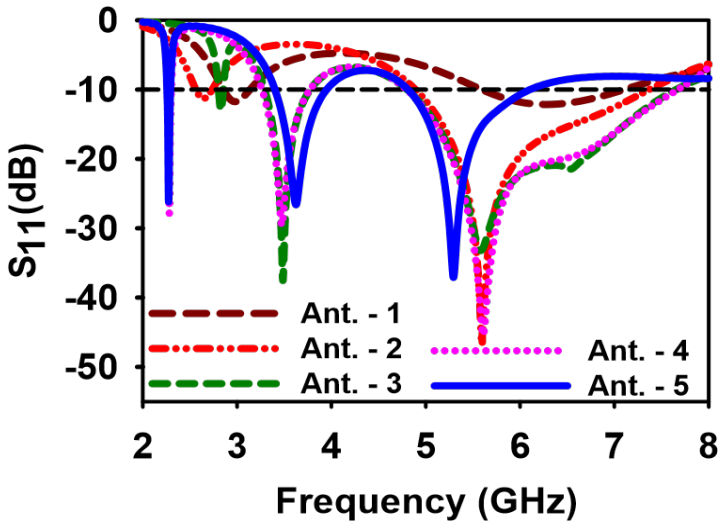

Figure 40-4 S_{11} responses of the antenna design stages described in Fig.40-3.

B. EQUIVALENT CIRCUIT MODELLING OF THE CRLH-TL ANTENNA-5

The proposed triple-band CRLH-TL loaded antenna pictured in Fig. 40-3(e) is based on open-ended boundary condition TL. The circuit model of the CRLH-TL antenna is pictured in Fig. 40-5. In the circuit diagram, the series arm mainly exists of a series inductor (L1) which is accounted due to the feedline part (Lf1 × Wf). The shunt capacitor C1 is represented by the asymmetric gap between the microstrip feed and AGP. Further CRLH-TL is loaded and which consists of a series capacitor represented by CL is formed due to the trimmed steptype

slot of gap G2. The series inductance (LR) is obtained due to Lf2 × Wf part which constitutes the series arm of CRLH-TL. For realizing shunt arm, chamfering is done in the normal meander line and it is represented by LL. The shunt capacitance (CR) is provided due to the gap between the chamfered meander lines. The additional capacitor (CV) is generated due to the coupling between triangular-shaped patch with edges that are blended and the AGP. Here the edge-blended triangular stub works as the virtual ground for the CRLH-TL antenna. The resistor (R) and conductance (G) accounts for the losses in TL. The intended antenna-5 is based on open-ended boundary condition of TL and hence the resonant frequency is due to shunt elements LL, CR, and CV.

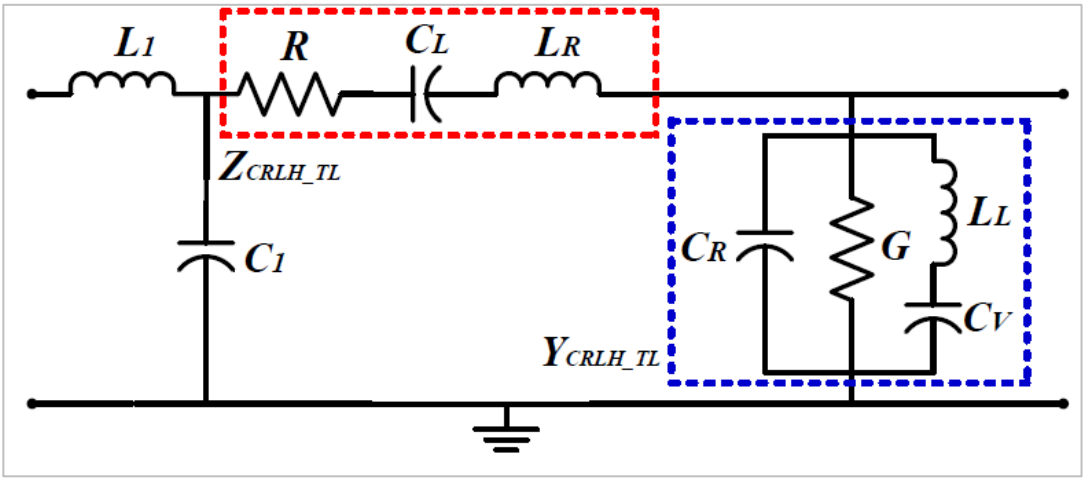

Figure 40-5 . Equivalent circuit diagram for the conformal CRLH-TL antenna-5

C. PARAMETRIC STUDIES OF THE INTENDED CRLH-TL ANTENNA

Fig. 40-6 shows the variation of the S11 responses by varying the series capacitor (CL) width represented by G2. It is noted that when the width G2 is varying from G2 = 0.1 mm to G2 = 0.9 mm and there is no variation in the ZOR. In Fig. 40-7, the variation of the shunt capacitor (CR) by changing the width W1 from W1 = 0.6 mm to W1 = 2.2 mm is depicted. It is clearly noted that the changes in the shunt element CR, the ZOR is shifting towards smaller frequency ranges and an optimized value of W1 = 1.8 mm is selected.

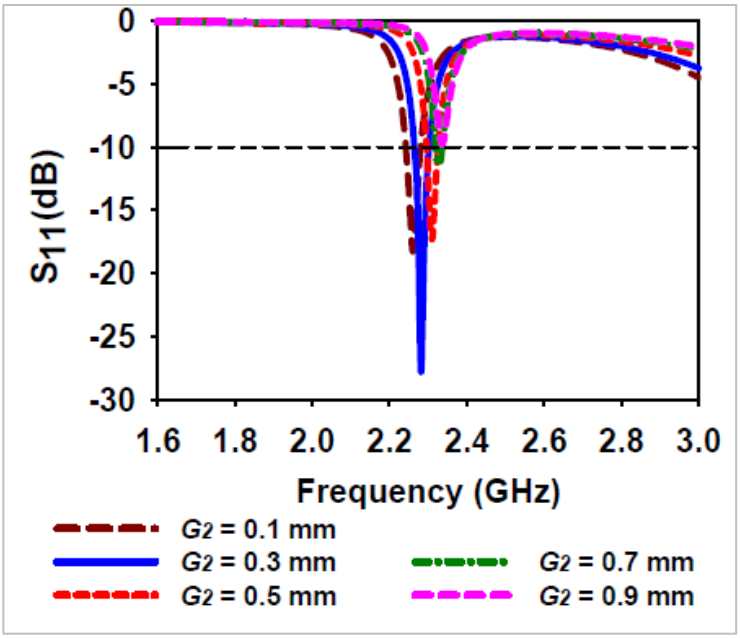

Figure 40-6 Simulated S_{11} of the Antenna-5 by varying G2 from 0.1 mm 0.9 mm.

Fig. 40-8 depicts the modification of shunt inductor (LL) values by varying the length L1 of the trimmed meander line. It is noted that by enlarging the length of the trimmed meander line from L1 = 4 mm to L1 = 8 mm. The resonance will shifts to a lower frequency range, signifies that increasing the shunt inductance (LL) shifts the resonance to smaller frequency and an optimized value of L1 = 6 mm is selected. So it is proved that changing the series and shunt parameters, the shift occurs in shunt elements and no shift is noticed by varying series elements.

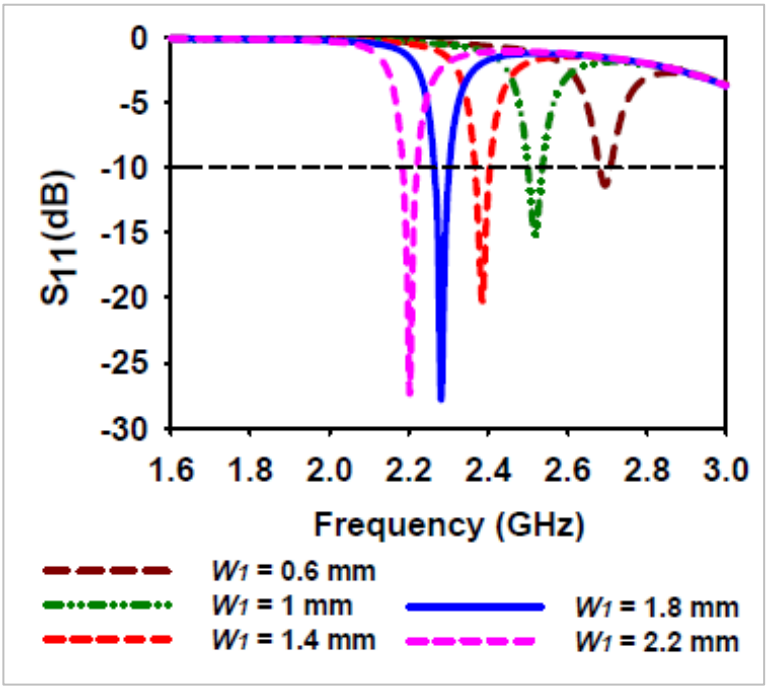

Figure 40-7 Simulated S_{11} of the Antenna-5 by varying W1 from 0.6 mm 2.2 mm.

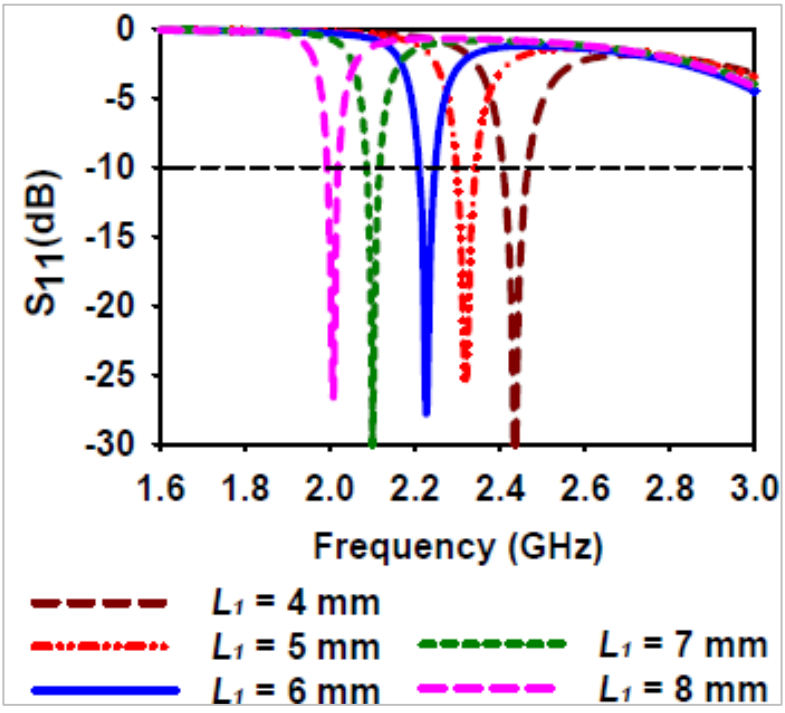

Figure 40-8 Simulated S_{11} of the Antenna-5 by varying L1 from 4 mm to 8 mm.

ANALYSIS OF CRLH-TL BASED CONFORMAL ANTENNA

The antenna-4 designed in the above stage can be made conformal by varying the θ as shown in Fig. 40-9 (antenna-5). By making conformal as depicted in Fig. 40-10 and 40-11, the antenna can be placed in any conformal surfaces with better space and volume utilization. Fig. 40-10(a) to 40-10(d) showing the antenna designs by changing the bending angle from $\theta = 30^0$ to $\theta = 120^0$. Also in Fig. 40-11(a) to 40-11(d) showing the antenna designs by changing the bending angle from $\theta = 150^0$ to $\theta = 240^0$. Fig. 40-12 and 40-13 depicts the variation of S_{11} characteristics from $\theta = 30^0$ to $\theta = 240^0$. It is to be noted that good S_{11} response are obtained at higher bending angle $\theta = 210^0$

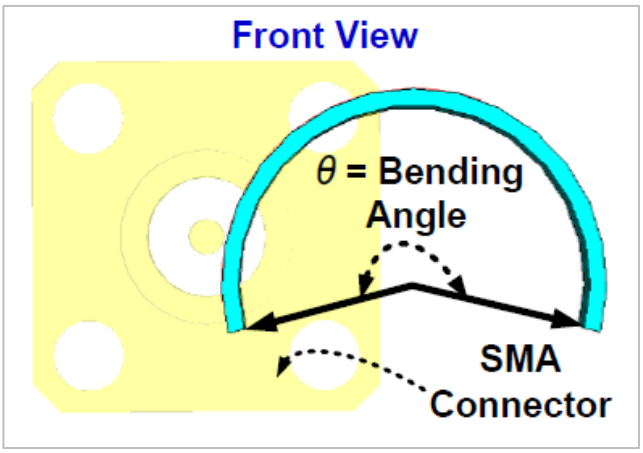

Figure 40-9 Proposed bending scheme with bending angle

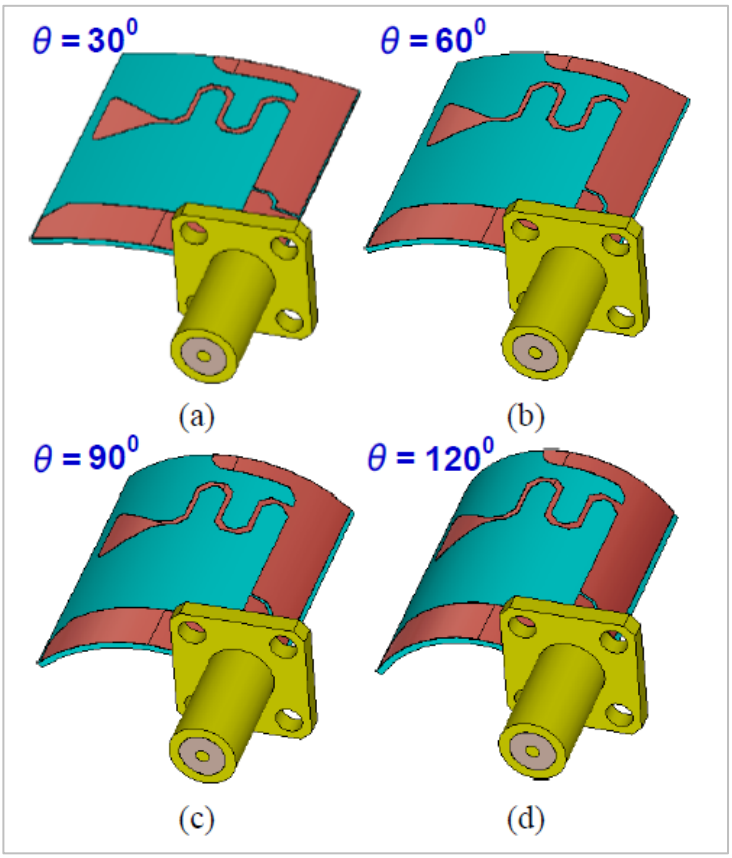

Figure 40-10 CRLH-TL based conformal antenna. (a) $\theta = 30^0$, (b) $\theta = 60^0$, (c) $\theta = 90^0$, and (d) $\theta = 120^0$

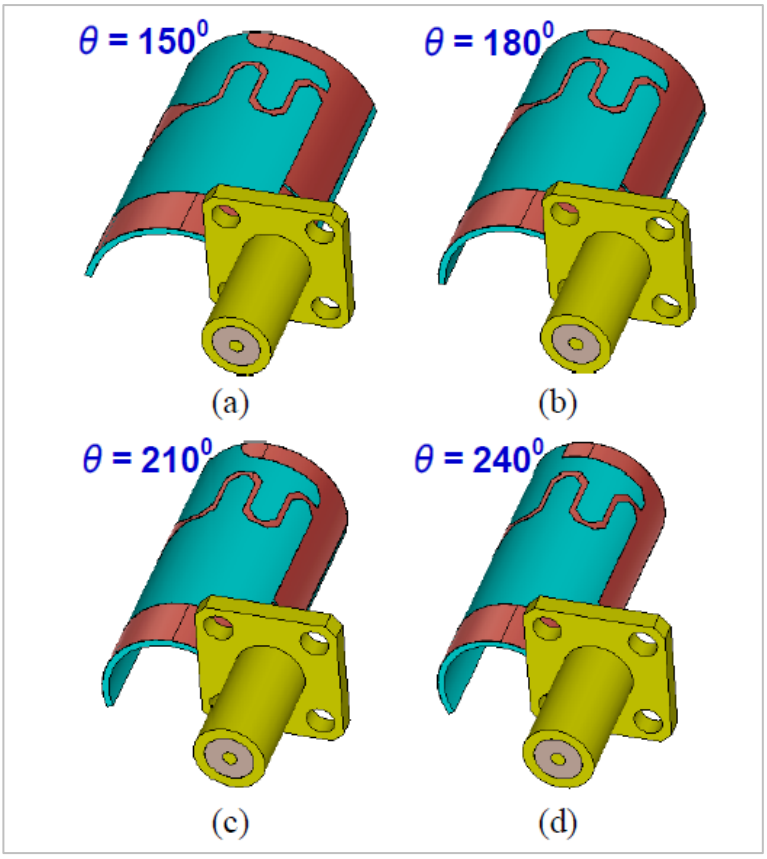

Figure 40-11 CRLH-TL based conformal antenna. (a) θ = 150⁰, (b) θ = 180⁰, (c) θ = 210⁰, and (d) θ = 240º

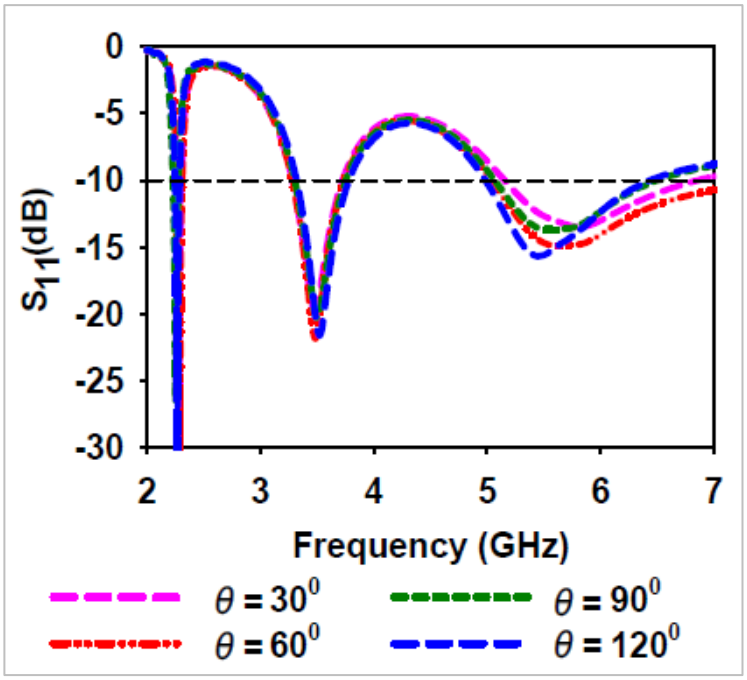

Figure 40-12 Simulated S_{11} results of the antenna-5 from θ =30⁰ to θ =120⁰

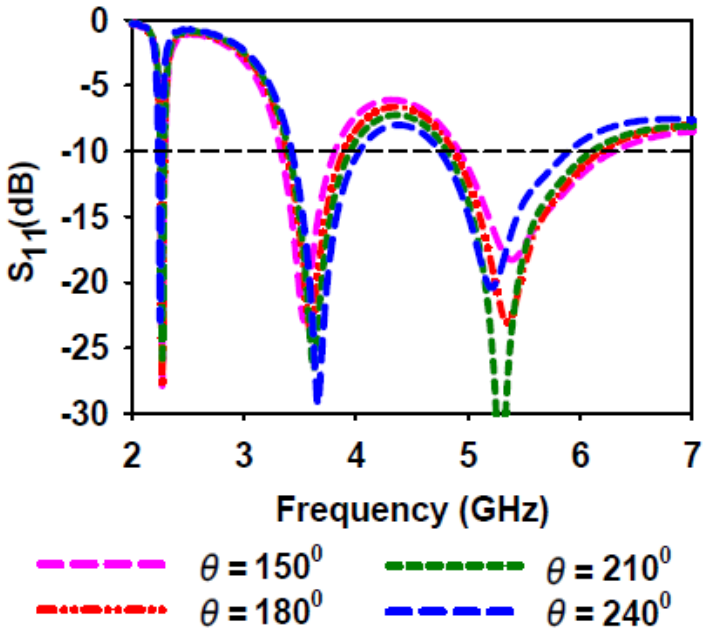

Figure 40-13 Simulated S_{11} results of the antenna-5 from $\theta = 150^0$ to $\theta = 240^0$

RESULTS AND DISCUSSIONS

The designed conformal antenna-5 is simulated using CST Microwave Studio. The 10-dB BW for the tri-band CRLH-TL antenna at $\theta = 210^0$ is 45 MHz (2.25–2.295 GHz), 564 MHz (3.39–3.954 GHz), and 1320 MHz (4.80–6.12 GHz) with an equivalent IBW of 1.98%, 15.62%, and 24.95% for the three consecutive bands at the mid frequencies of 2.27 GHz, 3.61 GHz, and 5.29 GHz as depicted in Fig. 40-14. Also, Fig. 40-15 demonstrates the radiation efficiency and gain of the intended antenna-5 at $\theta = 210^0$. The intended CRLH-TL conformal antenna exhibits a maximum gain of 0.76 dBi, 1.45 dBi and 3.22 dBi for the three consecutive bands. The simulated efficiency of 64.15%, 94.8%, and 97.02% is obtained for the working bands. The 2-D radiation pattern of the CRLH-TL antenna is also drawn. Fig. 40-16 depicts the simulated 2D patterns in *yz*– and *xz*–plane at the midpoints of each working band for 2.27 GHz, 3.61 GHz, and 5.29 GHz. For *xz*–plane at 2.27 GHz and 5.29 GHz, the antenna shows circular pattern and the bidirectional radiation behavior is noticed at 3.61 GHz. At *yz*– plane, bidirectional radiation behavior is noticed at 2.27 GHz and 5.29 GHz and circular pattern is observed at 3.61 GHz.

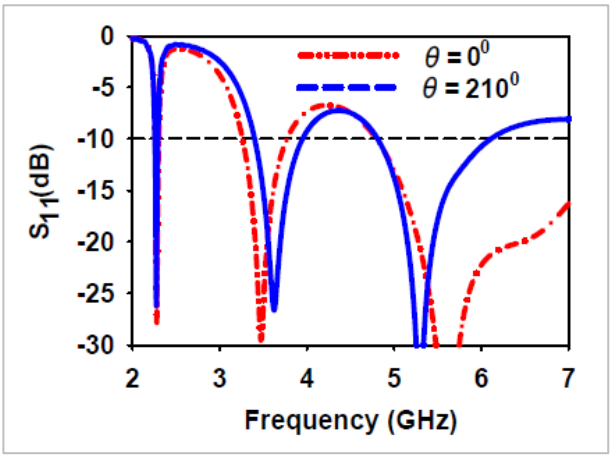

Figure 40-14 Simulated S_{11} response of the proposed tri-band CRLH-TL loaded antenna for $\theta = 0^0$ and $\theta = 210^0$

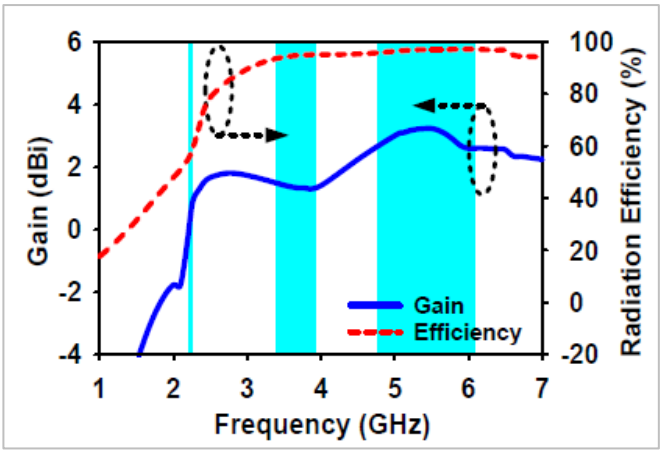

Figure 40-15 Gain and efficiency of the intended MTM antenna at θ =210^o

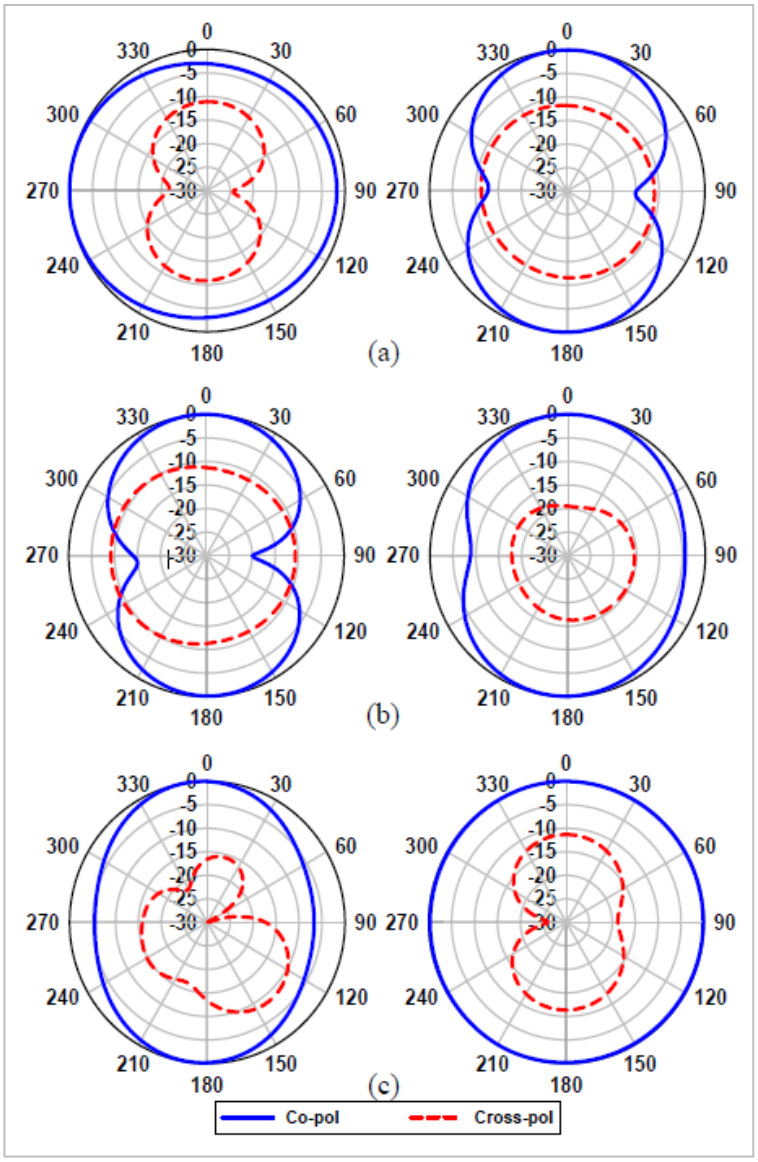

Figure 40-16 The radiation pattern of the conformal CRLH-TL antenna at θ = 210^0.

CONCLUSIONS

A compact CRLH-TL based low profile and miniaturized tri-band conformal antenna is designed and studied in this paper. The intended antenna shows improved IBW of 1.98%, 15.62% and 24.95% for the three consecutive frequency bands. The equivalent circuit model is designed and parametric investigations are done for analyzing the ZOR performance of the antenna. The intended antenna provides a compact electrical size of 0.17 λ_0 × 0.20 λ_0 × 0.004 λ_0 with ka = 0.84. Triple band antenna responses are obtained by simply changing the bending angle of the CRLH-TL antenna from $\theta = 0^0$ to $\theta = 210^0$.

REFERENCES

[1] A. Lai, K. et. al.,, "Infinite wavelength resonant antennas with monopolar radiation Pattern Based on Periodic Structures," IEEE Trans. Antennas Propag., vol. 55, no. 13, pp. 868–876, Mar. 2007.

[2] M. Ameen, S. Kalraiya and R. K. Chaudhary, "A compact low profile modified ACS-fed triple band open-ended metamaterial antenna for UMTS, WLAN, and WiMAX applications," 2019 URSI Asia-Pacific Radio Science Conference (AP-RASC), India, 2019, pp. 1–4.

[3] M. Ameen and R. K. Chaudhary, "Metamaterial circularly polarized antennas: Integrating an epsilon negative transmission line and single split ring-type resonator," IEEE Antennas Propag. Mag., .doi: 10.1109/MAP. 2019.2950920.

[4] M. Ameen and R. K. Chaudhary, "Metamaterial-based wideband circularly polarized antenna with rotated V-shaped metasurface for small satellite applications," Electron. Lett., vol. 55, no. 7, pp. 365–366, Apr. 2019.

[5] P. W. Chen and F. C. Chen, "Asymmetric coplanar waveguide (ACPW) zeroth-order resonant (ZOR) antenna with high efficiency and bandwidth enhancement," IEEE Antennas Wireless Propag. Lett., vol. 11, pp. 527–530, 2012.

[6] M. Ameen, and R. K. Chaudhary, "Metamaterial-based circularly polarised antenna employing ENG-TL with enhanced bandwidth for WLAN applications," Electron. Lett., vol. 54, no. 20, pp. 1152–1154, Oct. 2018.

[7] L. Liu and B. Wang, "A broadband and electrically small planar monopole employing metamaterial transmission line," IEEE Antennas Wireless Propag. Lett., vol. 14, pp. 1018–1021, 2015.

[8] P. L. Chi and Y. Shih, "Compact and bandwidth-enhanced zeroth-order resonant antenna," IEEE Antennas Wireless Propag. Lett., vol. 14, pp. 285–288, 2015.

[9] C. Zhou, G. Wang, J. Liang, et. al., "Broadband antenna employing simplified MTLs for WLAN/WiMAX Applications," IEEE Antennas Wireless Propag. Lett., vol. 13, pp. 595–598, 2014.

[10] M. Palandoken, A. Grede and H. Henke, "Broadband microstrip antenna with left-handed metamaterials," IEEE Trans. Antennas Propag., vol. 57, no. 2, pp. 331–338, Feb. 2009.

[11] L. M. Si, Q. L. Zhang, W. D. Hu, et al., "A uniplanar triple-band dipole antenna using complementary capacitively loaded loop," IEEE Antennas Wireless Propag. Lett., vol. 14, pp. 743–746, March 2015.

[12] L. Si, W. Zhu and H. Sun, "A compact, planar, and CPW-fed metamaterial-inspired dual-band antenna," IEEE Antennas Wireless Propag. Lett., vol. 12, pp. 305–308, 2013.

[13] W. Cao, et. al., "Multi-frequency and dual mode patch antenna based on electromagnetic band-gap (EBG) structure," IEEE Trans. Antennas Propag., vol. 60, no. 12, pp. 6007–6012, Dec. 2012

[14] M. S. Majedi and A. R. Attari, "A compact and broadband metamaterial-inspired antenna," IEEE Antennas Wireless Propag. Lett., vol. 12, pp. 345–348, 2013.

[15] J. Xiong, X. Lin, Y. Yu, et. al., "Novel flexible dual-frequency broadside radiating rectangular patch antennas based on complementary planar ENZ or MNZ metamaterials," IEEE Trans. Antennas Propag., vol. 60, no. 8, pp. 3958–3961, Aug. 2012.

[16] A. T. Castro and S. K. Sharma, "Inkjet-printed wideband circularly polarized microstrip patch array antenna on a PET film flexible substrate material," IEEE Antennas Wireless Propag. Lett., vol. 17, no. 1, pp. 176–179, Jan. 2018.

[17] S. M. Saeed, et. al., "Wearable flexible reconfigurable antenna integrated with artificial magnetic conductor," IEEE Antennas Wireless Propag. Lett., vol. 16, pp. 2396–2399, 2017.

[18] M. Wang, et. al., "Investigation of SAR reduction using flexible antenna with metamaterial structure in wireless body area network," IEEE Trans. Antennas Propag., vol. 66, no. 6, pp. 3076–3086, Jun. 2018.

[19] W. Li, Y. Hei, P. M. Grubb, X. Shi and R. T. Chen, "Compact inkjetprinted flexible MIMO antenna for UWB applications," IEEE Access, vol. 6, pp. 50290–50298, 2018.